Journal of Structural Geology, Vol. 11, No. 4, pp. 433 to 437, 1989
Printed in Great Britain

0191-8141/89 $03.00 + 0.00

Finite difference modelling of hangingwall deformation

DAVID WALTHAM

Department of Geology, Royal Holloway and Bedford New College, University of London, Egham Hill, Egham, Surrey TW20 0EX, U.K.

(*Received* 20 *August* 1988; *accepted in revised form* 22 *November* 1988)

Abstract—Modelling of hangingwall deformation, during extension or compression, may be achieved using a finite difference approach. Under the assumption of incompressible flow, equivalent to area balancing; this method enables calculation of a particle velocity field giving the trajectory of any point in the hangingwall during deformation. This technique is more flexible than graphical algorithms because it is not restricted to simple shear cases. Inputs to the algorithm are the bounding fault and the particle displacement directions. Simple examples are used to illustrate the method.

INTRODUCTION

MATHEMATICAL modelling of hangingwall deformation above a fault surface, during extension or compression, is an important problem in structural geology. Many investigators have developed methods based upon graphical techniques (Verrall 1982, Gibbs 1983, 1984, Davison 1986, White *et al.* 1986, Williams & Vann 1987, White 1988). These papers have been concerned with the forward problem of predicting deformation patterns and also the inverse problem of deriving fault geometry from observed deformation geometries. These approaches differ in their methods of accommodating deformation, e.g. vertical simple shear models (Verrall 1982, Gibbs 1983, 1984) and inclined simple shear models (White *et al.* 1986). However, recent work indicates that, in analogue models, deformation is more complex than these techniques allow (Ellis & McClay 1988, fig. 17).

This paper presents a forward modelling technique which can be applied to any form of incompressible deformation. The method is based upon finite difference solution of a partial differential equation, an approach familiar to programmers of seismic migration algorithms (Claerbout & Doherty 1972, Gazdag 1978, Berkhout 1981, Claerbout 1985). The general approach is to find a partial differential equation which must be satisfied by all forms of incompressible hangingwall deformation. A suitable partial differential equation is derived below. The problem then reduces to finding the particular solution corresponding to the situation being modelled. The finite difference method for finding such a solution is outlined in the third and fourth section. Finally, examples of its use are given.

THE GOVERNING EQUATION

Hangingwall deformation is completely described by a velocity field together with a deformation time. The velocity field gives the rate and direction of displacement for a particle at any point in the hangingwall. For example, a particle at the point A in Fig. 1 is displaced, during deformation, to the point B and, at the intermediate point (x, y), this particle moves at a displacement rate $v(x, y)$ in a direction $\theta(x, y)$ to the horizontal. These two quantities are more simply represented by the velocity vector $\mathbf{v}(x, y)$. This velocity field can be time dependent so that the path followed by a particle will not necessarily be the same as that of another particle occupying the same location at a different time.

The primary assumption of this paper is that of 'volume balancing', i.e. the material comprising the hangingwall is considered to be incompressible. The technique will therefore be inappropriate if significant compaction has occurred. The velocity field for motion of an incompressible 'fluid' must be solenoidal (Birkoff 1955, Hughes & Brighton 1967), i.e.

$$\nabla . \mathbf{v} = 0. \tag{1}$$

This condition ensures that the volume of material entering any fixed volume of space is equal to the volume of material leaving. For the case of a two-dimensional velocity field, equation (1) may be given in the form

$$\partial v_x/\partial x + \partial v_y/\partial y = 0. \tag{2}$$

Equation (2), being two-dimensional, will conserve the

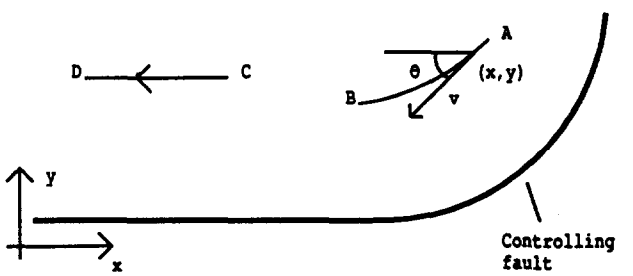

Fig. 1. Particle displacement geometry. During deformation, a particle at A in the hangingwall moves to the point B along the trajectory shown. At the intermediate point (x, y) this particle moves at a rate v in a direction θ to the horizontal. Thus, every point in the hangingwall has an associated displacement rate, v, and displacement direction, θ.

areas of beds rather than their volumes and so gives rise to an area balancing technique. Now, it is more convenient to describe the velocity field, $\mathbf{v}$, in terms of its amplitude, v, and direction, θ, using

$$v_x = v \cos(\theta) \quad (3)$$

$$v_y = v \sin(\theta). \quad (4)$$

Equation (2) can then be rewritten as

$$\partial v/\partial x + \tan(\theta)\, \partial v/\partial y = v(\tan(\theta)\, \partial\theta/\partial x - \partial\theta/\partial y). \quad (5)$$

This is the equation used in the finite difference algorithm developed in the next section.

Now, equation (5) is linear in v. The importance of this is that, for a given displacement direction field $\theta(x, y)$, the deformation will depend only upon the total extension, or compression, and not upon the rate at which it is achieved. In practice $\theta(x, y)$ will depend upon the strain rate and so the deformation geometry will differ according to the deformation rate. Nevertheless, this linearity will prove useful in the next section.

THE DIFFERENCE EQUATION

Thus far, θ and v have been treated as continuous functions of position. However, the finite difference solution gives these quantities only at discrete points on an x–y grid (see Fig. 2). This grid has m points in the x-direction and n points in the y-direction with sample intervals δx and δy, respectively. To simplify the notation, the grid locations will be specified by subscripts for the x-location and superscripts for the y-location. Hence, $v(i\delta x, j\delta y)$ is denoted v_i^j. The object of the finite difference algorithm is to calculate all the v_i^j and θ_i^j.

Thus, this algorithm has two parts. First, the displacement directions, θ_i^j, are given, this aspect is considered in the next section. Secondly, the displacement rates are calculated by finding a column of unknown displacement rates, $v_{i+1}^1, v_{i+1}^2, \ldots, v_{i+1}^n$ using the preceding column of displacement rates $v_i^1, v_i^2, \ldots, v_i^n$. The displacement rates, $v_1^1, v_1^2, \ldots, v_1^n$, in the first column of the finite difference grid must therefore be supplied. Fortunately,

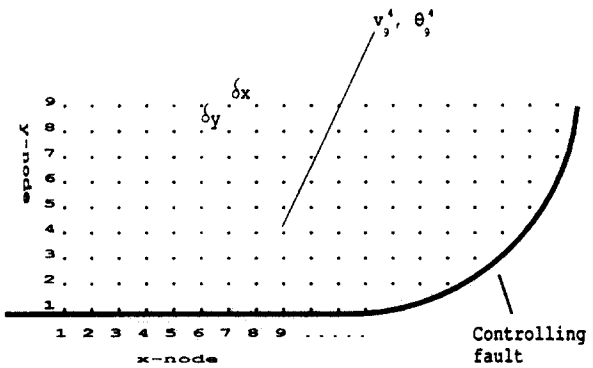

Fig. 2. Finite difference representation. The quantities v and θ are now only defined at discrete points which are separated by δx in the x-direction and δy in the y-direction. The values at each node of this grid are annotated with a subscript for the x-position of the node and a superscript for the y-position of the node.

because of the linearity already noted, these initial values may be set to unity. The deformation time is then adjusted to give the correct total extension or compression. This initial column of points then defines a hangingwall pin line (or loose line).

A simple algorithm for finding the column of unknown displacement rates could be devised as follows. The derivatives of displacement rate are first estimated from

$$(\partial v/\partial x)_i^j = (v_{i+1}^j - v_i^j)/\partial x$$

$$(\partial v/\partial y)_i^j = (v_i^{j+1} - v_i^j)/\partial y.$$

These are then substituted into equation (5) to yield

$$v_{i+1}^j = v_i^j(1 + [\tan(\theta)\, \partial\theta/\partial x - \partial\theta/\partial y]\delta x/\delta y + \tan(\theta)\, \delta x/\delta y) - v_i^{j+1} \tan(\theta)\, \delta x/\delta y.$$

Thus v_{i+1}^j, an element from the column of unknown values, is found from knowledge of θ together with v_i^j and v_i^{j+1} from the preceding column. Unfortunately this algorithm is numerically unstable, it produces very poor results and a more complex approach must be used. However, the basic idea of estimating the terms in equation (5) using values on the finite grid and then solving the resultant equation for the unknown elements, is still retained.

To produce numerically stable results the implicit finite difference scheme (Crank & Nicolson 1947, Claerbout 1985) is used. The crux of this method is that all quantities in the differential equation are estimated at points half-way between samples in the x-direction, i.e. at $(i + 1/2)\delta x, j\delta y$, giving:

$$v_{i+1/2}^j = (v_i^j + v_{i+1}^j)/2 \quad (6)$$

$$(\partial v/\partial x)_{i+1/2}^j = (v_{i+1}^j - v_i^j)/\delta x \quad (7)$$

$$(\partial v/\partial y)_{i+1/2}^j = [(v_i^{j+1} - v_i^{j-1}) + (v_{i+1}^{j+1} - v_{i+1}^{j-1})]/4\delta y \quad (8)$$

plus similar relations for θ. If these estimates are substituted into the partial differential equation, equation (5), then a set of linear simultaneous equations results. These may be expressed in matrix form, the $n = 5$ example being

$$\begin{bmatrix} a_{i+1/2} & \beta_{i+1/2}^1 & 0 & 0 & 0 \\ -\beta_{i+1/2}^2 & \alpha - \sigma_{i+1/2}^2 & \beta_{i+1/2}^2 & 0 & 0 \\ 0 & -\beta_{i+1/2}^3 & \alpha - \sigma_{i+1/2}^3 & \beta_{i+1/2}^3 & 0 \\ 0 & 0 & -\beta_{i+1/2}^4 & \alpha - \sigma_{i+1/2}^4 & \beta_{i+1/2}^4 \\ 0 & 0 & 0 & -\beta_{i+1/2}^5 & b_{i+1/2} \end{bmatrix} \begin{bmatrix} v_{i+1}^1 \\ v_{i+1}^2 \\ v_{i+1}^3 \\ v_{i+1}^4 \\ v_{i+1}^5 \end{bmatrix} = \begin{bmatrix} d_i^1 \\ d_i^2 \\ d_i^3 \\ d_i^4 \\ d_i^5 \end{bmatrix}, \quad (9)$$

where

$$\alpha = 1/\delta x$$

$$\beta_{i+1/2}^j = \tan(\theta_{i+1/2}^j)/4\, \delta y$$

$$\sigma_{i+1/2}^j = [(\tan(\theta)\, \partial\theta/\partial x - \partial\theta/\partial y)_{i+1/2}^j]/2$$

$$d_i^j = \beta_{i+1/2}^j\, v_i^{j-1} + (\alpha - \sigma_{i+1/2}^j)\, v_i^j - \beta_{i+1/2}^j\, v_i^{j+1}$$

and the values of $a_{i+1/2}$, $b_{i+1/2}$, d_i^1 and d_i^n depend upon the boundary conditions. In the examples given in this paper it is assumed that the displacement rate gradient is zero at the boundaries, i.e. $v_i^0 = v_i^1$ and $v_i^{n+1} = v_i^n$. These conditions lead to

$$a_{i+1/2} = (\alpha - \sigma - \beta)_{i+1/2}^1 \quad (10)$$

$$b_{i+1/2} = (\alpha - \sigma + \beta)_{i+1/2}^n \quad (11)$$

$$d_i^n = v_i^{n-1}\,\beta_{i+1/2}^n + v_i^n(\alpha - \sigma - \beta)_{i+1/2}^n \quad (12)$$

Hence, all matrix elements, in equation (9), may be calculated from the known direction field. In addition, the right-hand vector elements are known and thus inversion of equation (9) yields the unknown quantities, v_{i+1}^j. Fast algorithms for solving systems of tridiagonal equations, such as equation (9), are widely reported in the literature (e.g. Claerbout 1985).

Once the displacement rate and direction have been found the deformation is calculated as follows. The hangingwall is deformed for a short time, δt, by calculating the displacement of points within it. For example, a point at (x, y) moves to $(x + v_x\,\delta t, y + v_y\,\delta t)$. This procedure is repeated N times, where $N\,\delta t$ equals the total time for which deformation occurs. This deformation time is calculated from the total extension, or compression, assuming unit displacement rate for the pin line. The time increment, δt, should be sufficiently small that the particle's true curved trajectory is closely approximated by the resultant set of straight line segments. The speed of the algorithm is largely controlled by the velocity field calculation and is not therefore significantly improved by using a larger time step. Note that a particle moving along a trajectory during deformation will not necessarily sit exactly at a point on the finite difference grid, at any given moment, but will lie at an intermediate position. Thus, calculation of the particle trajectory will require interpolation of the velocity field found by the finite difference technique.

THE DIRECTION FIELD

It has been assumed that the directions, θ_i^j, are known. Hangingwall deformation will be controlled by this displacement direction field which is constrained only by the requirement that displacement be parallel to the bounding fault at points close to the fault. Some simple direction fields which obey this constraint will now be discussed.

The simplest assumption is to make displacement direction parallel to the fault dip vertically beneath the point in question. This is vertical simple shear which gives the same results as those from the simplest graphical techniques (e.g. Verrall 1982).

Alternatively, the directions can be parallel to the fault in some non-vertical direction. This is the inclined simple shear assumption and will give results equivalent to those of White *et al.* (1986).

A different way of viewing these direction fields is to consider the corresponding displacement isogons (see Fig. 3). Displacement isogons are contours of the displacement direction, i.e. lines joining points with equal values for θ. Vertical simple shear corresponds to isogons which are vertical straight lines whilst inclined simple shear has inclined straight isogons. In general, the isogons can have any curved non-intersecting form, the value of θ on any isogon being equal to the fault dip at the intersection of isogon and fault. This approach suggests a more sophisticated assumption for θ in which the dip of the isogons depends upon depth. Alternatively, the isogon dip could depend upon the materials comprising the hangingwall. For an inhomogeneous hangingwall the direction field would then have to be recalculated after each increment of displacement.

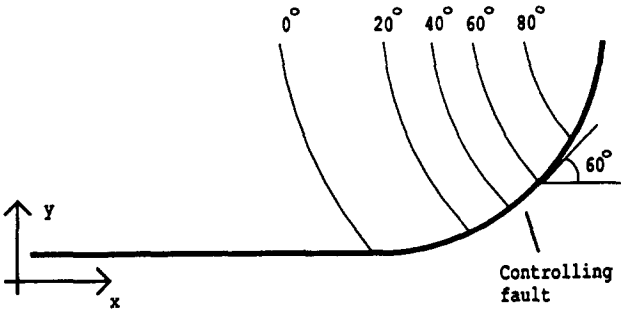

Fig. 3. Displacement direction isogons. Each contour joins points of equal displacement direction. These displacement directions must be parallel to the fault for points on the fault. This is indicated for the 60° isogon.

SIMPLE EXAMPLES

Figure 4 illustrates a simple example of the use of this algorithm. The hangingwall has been moved by 4.5 km above a simple listric detachment. The pre-rift sediments in this hangingwall are represented by a 0.5 km square grid of points which was successively deformed by extension in increments of 100 m (N.B. this grid of points is not related to the finite difference grid already discussed). Syn-rift deposits are represented by introducing a new horizontal layer of points after every 1 km of extension. A direction field was used in which the isogons were assumed to be straight lines dipping by 20° anticlockwise from vertical.

This example illustrates well the simulation of features such as a roll over geometry and wedge shaped growth intervals in the syn-rift sediments. It also shows that area balancing can produce elongation of the pre-rift sediments and that this algorithm does not reproduce faulting.

Figure 5 shows uniform extension on a ramp/flat style fault. The hangingwall pin line has been moved a total of 6 km. Pre-rift sediments are here represented by a 1 km square grid of points and the syn-rift sediment layers have been deposited after each 0.5 km of extension. The direction field again used 20° dipping isogons.

In addition to the features observed in Fig. 4, this example shows a hangingwall syncline and an unfolding roll over in the syn-rift layers giving rise to a prograding

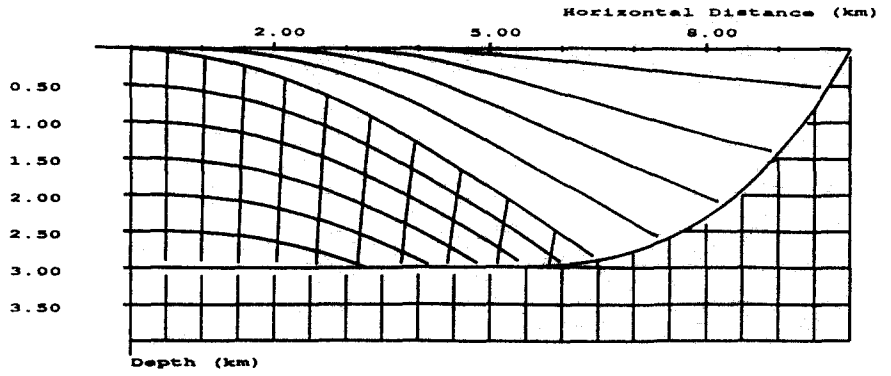

Fig. 4. Simple listric example after 4.5 km of extension. The distorted grid represents pre-rift sediments. Syn-rift sediments have been represented by introducing a line of points at the surface after each 1 km of extension.

appearance. The apparent faulted structure in the syn-rift deposits is actually a locus of points which have passed through $x \sim 14$ km, $z \sim 0$ km which is a point of low displacement rate. Consequently the syn-rift layers are very close to one another at these points.

DISCUSSION

A hangingwall deformation modelling technique has been presented which allows any form for the particle displacement directions. Thus, great flexibility in attempting to model true geological situations is possible. Simple examples have been given which could have been produced using simpler graphical techniques, but the algorithm is by no means restricted to such cases. Further work is now in progress to find and test other possibilities, the results of this will be reported in a subsequent paper.

An important facet of this will be the ability to use time-dependent direction fields since, in practice, deformation is accommodated by faulting which moves with the hangingwall. Time-independent modelling, on the other hand, produces deformation in a manner which is stationary with respect to the footwall. Thus, an ideal modelling scheme must allow the direction field to evolve as deformation proceeds.

An aspect not considered in this paper is that of modelling in three dimensions. Equation (1) however is a full three-dimensional statement. Thus, in principle, the techniques presented here should extend to three dimensions although the practical problems will not be trivial.

A further aspect not considered here is the problem of estimating fault geometry from known hangingwall deformation, i.e. the inverse problem. This is related to the problem of estimating the displacement directions rather than assuming them. Thus, at present the only method available would be to adapt iteratively a forward model until it gave results consistent with the known deformation. There would then be a serious problem of non-uniqueness, a problem avoided with graphical techniques because of their extremely restricted choice of direction fields.

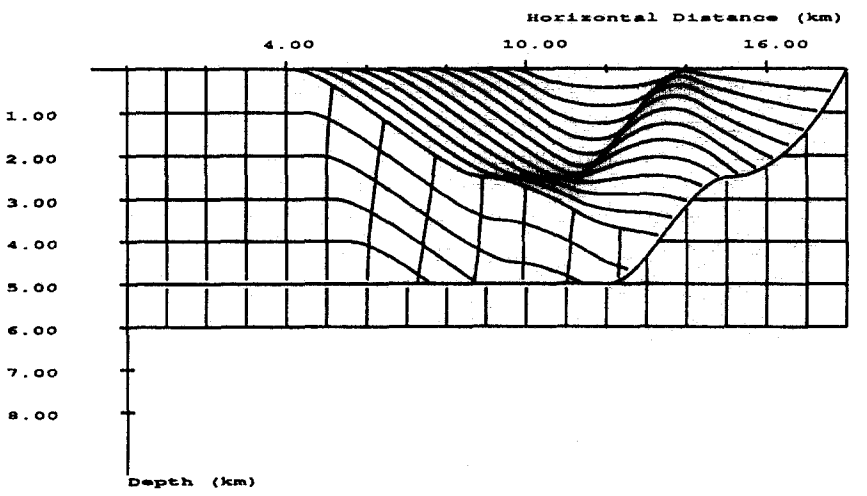

Fig. 5. Ramp/flat controlling fault with 6 km of extension. Syn-rift points have been deposited every 0.5 km in this example.

Acknowledgements—I should like to thank Drs Ken McClay and Mike Norton of RHBNC geology department for their helpful comments on this work. This research was conducted as part of NERC project GR3/6658.

REFERENCES

Berkhout, A. J. 1981. Wave field extrapolation techniques in seismic migration, a tutorial. *Geophysics* **46**, 1638–1656.

Birkoff, G. 1955. *Hydrodynamics*. Dover Publications, New York.

Claerbout, J. F. 1985. *Imaging the Earth's Interior*. Blackwell Scientific, Oxford.

Claerbout, J. F. & Doherty, S. M. 1972. Downward continuation of moveout corrected seismograms. *Geophyics* **37**, 741–768.

Crank, J. & Nicolson, P. 1947. A practical method for numerical evaluation of solutions of partial differential equations of the heat-conduction type. *Proc. Cambridge Phil. Soc.* **43**, 50.

Davison, I. 1986. Listric normal fault profiles: calculation using bed-length balance and fault displacement. *J. Struct. Geol.* **8**, 209–210.

Ellis, P. G. & McClay, K. R. 1988. Listric extensional fault systems—results of analogue model experiments. *Basin Res.* **1**, 55–70.

Gazdag, J. 1978. Wave equation migration with the phase shift method. *Geophysics* **43**, 1342–1351.

Gibbs, A. D. 1983. Balanced cross-section constructions from seismic sections in areas of extensional tectonics. *J. Struct. Geol.* **6**, 152–160.

Gibbs, A. D. 1984. Structural evolution of extensional basin margins. *J. geol. Soc. Lond.* **141**, 609–620.

Hughes, W. F. & Brighton, J. A. 1967. *Theory and Problems of Fluid Dynamics*. McGraw-Hill, New York.

Verrall, P. 1982. Structural interpretation with applications to North Sea problems. Course Notes No. 3. JAPEC.

White, N. J., Jackson, J. A. & McKenzie, D. P. 1986. The relationship between the geometry of normal faults and that of sedimentary layers in their hangingwalls. *J. Struct. Geol.* **8**, 897–910.

White, N. J. 1988. Extension and subsidence of the continental lithosphere. Unpublished Ph.D thesis, University of Cambridge.

Williams, G. & Vann, I. 1987. The geometry of listric normal faults and deformation in their hangingwalls. *J. Struct. Geol.* **9**, 789–795.